Developmental Cell
Short Article

Ter94 ATPase Complex Targets K11-Linked Ubiquitinated Ci to Proteasomes for Partial Degradation

Zhao Zhang,[1] Xiangdong Lv,[1] Wen-chi Yin,[2] Xiaoyun Zhang,[2] Jing Feng,[1] Wenqing Wu,[1] Chi-chung Hui,[2] Lei Zhang,[1,*] and Yun Zhao[1,*]
[1]State Key Laboratory of Cell Biology, Institute of Biochemistry and Cell Biology, Shanghai Institutes for Biological Sciences, Chinese Academy of Sciences, Shanghai 200031, China
[2]Program in Developmental and Stem Cell Biology, The Hospital for Sick Children and Department of Molecular Genetics, University of Toronto, Toronto, ON M5G 1L7, Canada
*Correspondence: rayzhang@sibcb.ac.cn (L.Z.), yunzhao@sibcb.ac.cn (Y.Z.)
http://dx.doi.org/10.1016/j.devcel.2013.05.006

SUMMARY

The Cubitus interruptus (Ci)/Gli family of transcription factors can be degraded either completely or partially from a full-length form (Ci155/Gli^{FL}) to a truncated repressor (Ci75/Gli^{R}) by proteasomes to mediate Hedgehog (Hh) signaling. The mechanism by which proteasomes distinguish ubiquitinated Ci/Gli to carry out complete versus partial degradation is not known. Here, we show that Ter94 ATPase and its mammalian counterpart, p97, are involved in processing Ci and Gli3 into Ci75 and Gli3^{R}, respectively. Ter94 regulates the partial degradation of ubiquitinated Ci by Cul1-Slimb-based E3 ligase through its adaptors Ufd1-like and dNpl4. We demonstrate that Cul1-Slimb-based E3 ligase, but not Cul3-Rdx-based E3 ligase, modifies Ci by efficient addition of K11-linked ubiquitin chains. Ter94$^{Ufd1\text{-}like/dNpl4}$ complex interacts directly with Cul1-Slimb, and, intriguingly, it prefers K11-linked ubiquitinated Ci. Thus, Ter94 ATPase and K11-linked ubiquitination in Ci contribute to the selectivity by proteasomes for partial degradation.

INTRODUCTION

Hh signaling plays important roles in metazoan development, and its malfunction is implicated in numerous human congenital disorders and cancers. Secreted Hh proteins bind Patched (Ptc)-iHog coreceptors to relieve an inhibitory effect of Ptc on Smoothened (Smo), which leads to activation of the Ci/Gli family of zinc finger transcription factors (Chen et al., 2007; Hooper and Scott, 2005; Jiang and Hui, 2008). Biochemical and genetic studies in *Drosophila* have revealed several important steps in the regulation of Ci/Gli activity (Hui and Angers, 2011) (Figure 1A). In the absence of Hh, full-length Ci, Ci155, is sequentially phosphorylated by protein kinase A (PKA), glycogen synthase kinase 3 (GSK3), and casein kinase I (CKI) and then ubiquitinated by Cullin 1 (Cul1)-Supernumerary limbs (Slimb, known also as β-TrCP)-based E3 ligase. This results in partial degradation by proteasomes, leaving the N terminus of Ci intact (Ci75) as a transcriptional repressor (Aza-Blanc et al., 1997; Jia et al., 2002; Price and Kalderon, 2002). In the presence of Hh, unphosphorylated Ci155 accumulates and enters nucleus to activate Hh target genes. As a feedback control of the pathway, active Ci155 induces the expression of *roadkill* (*rdx*)/*Hib* to form Cul3-Rdx-based E3 ligase and promotes complete proteasomal degradation of Ci155 (Kent et al., 2006; Zhang et al., 2006).

Although it is well established that Ci is ubiquitinated by Cul1-Slimb and Cul3-Rdx-based E3 ligases under different conditions, it remains unknown how proteasomes distinguish ubiquitinated Ci for partial versus complete degradation. As ubiquitinated proteins are transferred to proteasomes by different pathways (Hartmann-Petersen et al., 2003), we hypothesize that some specific components are involved in the recruitment of ubiquitinated Ci for partial degradation. Transitional elements of the endoplasmic reticulum 94 kDa (Ter94) (Pintér et al., 1998) was identified as the *Drosophila* homolog of yeast CDC48, which is a member of the ATPase associated with various cellular activities (AAA) family. In mammals, the CDC48/Ter94 homolog p97 (also known as VCP) mainly functions in endoplasmic reticulum-associated degradation (ERAD) (Meyer et al., 2012; Richly et al., 2005; Ye et al., 2001). Proteomic analysis revealed that p97 might play a broad role in regulating the turnover of ubiquitin proteasome system (UPS) substrates (Alexandru et al., 2008). Here, we showed that Ter94 is a component of the Ci processing machinery and is critical for Ci75 formation.

RESULTS

Ter94/p97 Regulates Partial Degradation of Ci155/Gli3 through Its ATPase Activity

To investigate the potential role for Ter94 in Ci regulation, we used the heritable RNAi technique to inactivate Ter94 (Figures S1A and S1B–S1C′ available online). By immunostaining *Drosophila* wing discs (Figure 1B) using Ci 2A1 antibody (Motzny and Holmgren, 1995), which recognizes only full-length Ci155 (Figure 1C), we found that *Ter94* knockdown (marked by GFP expression in *Act5c > CD2 > Gal4 (AG4)-Dicer2-GFP* flies) leads to accumulation of Ci155 (Figures 1D and 1D′, arrows), although not all *Ter94* RNAi clones showed the same level of Ci

accumulation (Figures 1D and 1D′, arrowheads showed a mild increase of Ci155). We next used the "Minute FRT" approach (Simpson, 1979) to generate *Ter94*^{k15502} clones lacking endogenous Ter94, which are generally small in size due to the role for Ter94 in growth. Consistent with the notion that Ter94 is essential for Ci degradation, *Ter94*^{k15502} clones also accumulated high levels of Ci155 (Figures 1E and 1F″, arrows). Elevated levels of Ci155 are not caused by increased *ci* transcription as the expression of *ci-lacZ*, an enhancer trap that recapitulates *ci* transcription (Eaton and Kornberg, 1990), was not affected by *Ter94* RNAi (Figures 1G–1G‴).

We next examined the effect of *Ter94* knockdown in eye discs, in which cells anterior to the morphogenetic furrow (MF) do not receive any Hh signal produced by cells posterior to the MF (Ou et al., 2002). Interestingly, Ci155 accumulated only in *Ter94* RNAi cells anterior to the MF (Figures 1H and 1I), suggesting that Ter94 regulates Ci155 levels in the absence of Hh signaling. An ATP-binding mutant of Ter94 (Ter94^{AA}) was made according to human p97^{AA} mutant (Ye et al., 2003). Similar to those observed in *Ter94* knockdown discs, overexpression of Ter94^{AA}-V5 resulted in Ci155 accumulation in wing discs (Figures S1D–S1D″) and eye discs (Figures 1J and 1K). These observations suggest that Ter94^{AA} acts as a dominant-negative mutant to interfere with endogenous Ter94 function and indicate that the ATPase activity of Ter94 is essential for Ci regulation. The ratio of Ci155 to Ci75 was dramatically increased (from 0.32 to 1.40) upon knockdown of *Ter94* in HA-Ci155-expressing wing discs (Figure 1L), indicating a specific role of Ter94 in the partial degradation of Ci.

To further investigate the physiological role of Ter94 in Ci75 formation, we examined the expression of *dpp*, which is a known target of Ci75 repressor (Aza-Blanc et al., 1997; Méthot and Basler, 1999). *Ter94* knockdown resulted in a notable accumulation of Ci155, no obvious upregulation of *dpp-lacZ* was observed (Figures S1E–S1F′). As knockdown of *Ter94* is incomplete (Figure S1A) due to the abundance of Ter94 in cells, the residual Ci75 may still block *dpp* expression. To get a clean answer to this question, we employed *Ter94*^{K15502} mutant clones. As shown in Figures 1M and 1N, *dpp-lacZ* expression was upregulated in some *Ter94*^{K15502} mutant clones. As processing of Ci155 to Ci75 is compromised in *Ter94* knockdown wing discs as revealed by western blot analysis (Figure 1L), and Ci75 is a known repressor of *dpp*, these observations together provide indirect evidence suggesting that Ci75 is absent in cells lacking Ter94 leading to derepression of *dpp-lacZ* and that loss of Ci processing in these cells results in elevated Ci155 levels. We noticed that some large *Ter94*^{K15502} mutant clones around the dorsal part of the anterior/posterior boundary instead exhibited reduced *dpp-lacZ* expression (Figure 1M), suggesting that *dpp-lacZ* regulation is complex and Ter94 may influence other factors that contribute to *dpp-lacZ* expression.

Among the three Gli proteins, Gli3 is processed efficiently into a truncated Gli3^{R} form, similar to Ci75 (Wang et al., 2000). We explored whether p97, the mammalian counterpart of Ter94, is involved in the proteolytic processing of Gli3. Knockdown of *p97* in NIH/3T3 cells stabilized Gli3^{FL} but reduced the levels of Gli3^{R} (Figure 1O). The ratio of Gli3^{FL} to Gli3^{R} increased from 0.40- to 1.03-fold upon knockdown of *p97* (Figure 1O). Furthermore, the ATPase activity of p97 is also critical for Gli3 processing. In NIH/3T3 cells, p97^{WT} overexpression did not alter the processing of Gli3, whereas expression of the ATP-binding mutant p97^{AA} (Ye et al., 2003) blocked Gli3^{R} formation in a dose-dependent manner (Figures S1J and S1K). Consistent with the reduction of Gli3^{R} levels, the activity of the 8xGliBS reporter was also significantly increased by overexpression of p97^{AA} but not p97^{WT} (Figure S1L). These results illustrate an evolutionarily conserved role of p97 in the partial degradation of Gli3.

In addition to proteasomal degradation, p97/VCP is also involved in endosomal trafficking and autophagy (Meyer et al., 2012). We tested the knockdown effects of *Hrs*, a component of the ESCRT-0 protein complex that mediates endosomal trafficking (Henne et al., 2011), on Ci levels. As shown in Figures S1G–S1G′, Ci levels were not altered in *Hrs* knockdown clones suggesting that the knockdown effect of *Ter94* on Ci is not related to endosomal trafficking. We next examined the requirement of Vps34, which is a critical component of autophagy (Juhász et al., 2008), on Ci regulation and found that *Vps34*$^{\Delta m22}$ clones lacking Vps34 function exhibit similar levels of Ci comparable to wild-type cells (Figures S1H–S1I). These results suggest that the regulation of Ci stability by Ter94 is not dependent on endosomal trafficking or autophagy.

Loss-of-Ter94 Function Blocks Ci Degradation by Cul1-Slimb-Based E3 Ligase, Not by Cul3-Rdx-Based E3 Ligase

We next examined the effects of *Ter94* knockdown on Ci degradation by Cul1-Slimb-based E3 ligase. Although overexpression of Flag-Slimb downregulated Ci155 levels in cells anterior to the MF of the eye disc (Figures 2A–2B″), simultaneous expression of Flag-Slimb and *Ter94* RNAi led to an accumulation of Ci155 (Figures 2C–2D″). These observations suggest that Ter94 acts downstream of Cul1-Slimb-based E3 ligase to regulate Ci degradation.

Unlike in the eye disc, Ci is only expressed in the anterior compartment of the wing disc. Hh expressed by posterior cells diffuses to anterior cells, causing differential phosphorylation of Ci leading to its stabilization in the anterior/posterior boundary and its degradation in the anterior compartment (Hooper and Scott, 2005). *UAS-Flag-Slimb* expression driven by *MS1096* in the wing pouch downregulated Ci155 mainly in the anterior compartment away from the anterior/posterior boundary (Figures 2E–2G). However, Ci155 still accumulated in anterior *Ter94*^{K15502} mutant clones when Flag-Slimb was overexpressed (Figures 2H–2I′). Based on these results, we conclude that Ter94 acts downstream of Cul1-Slimb-based E3 ligase to promote Ci degradation.

Cul3-Rdx-based E3 ligase promotes Ci degradation in the presence of Hh signaling (Kent et al., 2006; Ou et al., 2002; Zhang et al., 2006). In the eye discs, overexpression of Flag-Rdx downregulated Ci155 in cells both anterior to the MF and posterior compartment (Figures S2A–S2B″). However, Ci155 degradation was not blocked when Flag-Rdx and *Ter94* RNAi were overexpressed together (Figures S2C–S2D″). Similarly, Flag-Rdx overexpression in the wing disc downregulated Ci155 levels (Figures S2E–S2G) and no obvious accumulation of Ci155 was observed when Flag-Rdx was overexpressed in *Ter94*^{K15502} mutant clones (Figures S2H–S2I′). These data

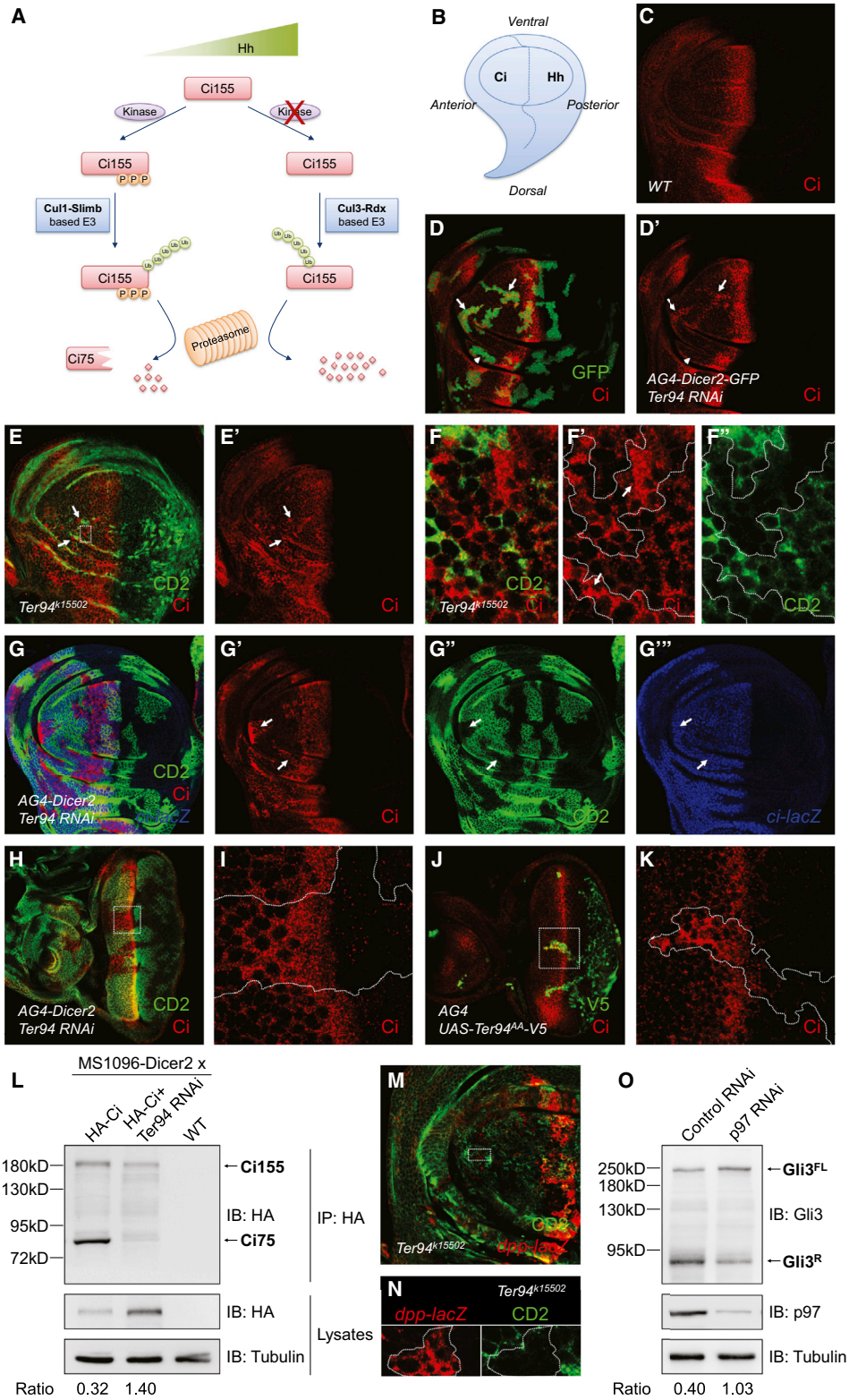

Figure 1. Ter94/p97 Regulates the Stability of Ci155/Gli3 through Its ATPase Activity

(A) A schematic drawing shows the regulation of Ci by dual ubiquitination systems.

(B) A cartoon of *Drosophila* third-instar larval wing disc. Hh is expressed in the posterior compartment and diffuses to the anterior compartment to form an Hh signaling gradient, whereas Ci is only expressed in the anterior compartment.

(C) Immunostaining of a wild-type (WT) wing disc using the Ci 2A1 antibody, which only recognizes Ci155 (red).

(legend continued on next page)

indicate that loss-of-Ter94 does not influence Cul3-Rdx-mediated Ci degradation.

Ter94$^{Ufd1\text{-}like/dNpl4}$ Complex Interacts with Cul1-Slimb-Based E3 Ligase via the Binding of Ufd1-like and Roc1a

The diverse functions of p97 are dictated by various adaptor proteins, such as Ufd1/Npl4, that are involved in the ERAD process (Ye, 2006). We predicted that the *Drosophila* homologs of Ufd1/Npl4 adaptors, Ufd1-like/CG4673, could form a functional complex with Ter94 in the regulation of Ci stability. By coimmunoprecipitation (coIP) experiments, we showed that Flag-Ufd1-like and Flag-CG4673 form a complex with Ter94-V5 in S2 cells (Figure 3A). Importantly, similar to that observed in *Ter94* knockdown, knockdown of *Ufd1-like* or *CG4673* also resulted in Ci155 accumulation in vivo (Figures 3B–3E). Based on conservation and functional similarity of CG4673 and Npl4 (data not shown), we named CG4673 as *Drosophila* Npl4 (dNpl4). As a control, we showed that knockdown of *p47*, which is another adaptor of p97 that functions in membrane fusion (Kondo et al., 1997), does not affect the stability of Ci155 (Figure 3F). These findings suggest that Ter94 forms a complex with its adaptors Ufd1-like/dNpl4 to regulate Ci degradation.

To investigate whether Ter94$^{Ufd1\text{-}like/dNpl4}$ interacts with Cul1-Slimb-based E3 ligase, we performed coIP experiments to show that Ter94-V5 forms complexes with 3xFlag-Cul1 and 3xFlag-Slimb (Figure 3G). To elucidate the interactions between Ter94$^{Ufd1\text{-}like/dNpl4}$ and the Cul1-Slimb-based E3 ligase, we carried out a series of GST pull-down experiments (Figures 3H, S3A, and S3B). Components of the Cul1-Slimb-based E3 ligase (see verification of the Cul1-Slimb complex in Figures S4A and S4B) (Cardozo and Pagano, 2004; Murphy, 2003; Noureddine et al., 2002) as well as the Ter94$^{Ufd1\text{-}like/dNpl4}$ complex were purified from *Escherichia coli* and used to screen for potential interactions. Our results showed that Roc1a interacts directly with Ufd1-like (Figure 3H) in vitro. Furthermore, this interaction was verified in S2 cells by coIP (Figure 3I).

We performed a two-step immunoprecipitation experiment to determine whether Ter94-Ufd1-like and Ufd1-like-Roc1a are in two different complexes or they could form a larger complex in cells. As shown in Figure 3J, Ter94-V5 was found in both 3xFlag-Roc1a and T7-Ufd1-like immunoprecipitates, indicating that Roc1a, Ufd1-like, and Ter94 form a complex, and that Cul1-Slimb-based E3 ligase could form a larger complex with Ter94$^{Ufd1\text{-}like/dNpl4}$ through the interaction between Ufd1-like and Roc1a.

K11-Linked Ubiquitin Chains Are Added on Ci by Cul1-Slimb-Based E3 Ligase

As ubiquitinated Ci155 by Cul1-Slimb or Cul3-Rdx-based E3 ligase has different destiny, it raises a possibility that ubiquitin chains linked on Ci155 by Cul1-Slimb or Cul3-Rdx-based E3 ligase may be different. To test this, we purified Cul1-Slimb as well as Cul3-Rdx-based E3 ligase (see verification of Cul3-Rdx complex in Figure S4C) (Donaldson et al., 2004; Ou et al., 2002; Zhang et al., 2006) from S2 cells (see verification of purified Cullin complex in Figures S4D and S4E) and performed in vitro ubiquitination on purified GST-Ci from *E. coli* (Figure 4A). Mass spectrometry (MS) analysis revealed that Cul1-Slimb and Cul3-Rdx-based E3 ligases added a similar but smaller amount of K63-linked ubiquitin chains, which are implicated in signal transduction, receptor endocytosis, and DNA-repair (Haglund and Dikic, 2005), to Ci (Figure 4B). In contrast, Cul3-Rdx-based E3 ligase mainly added K48-linked ubiquitin chains (81.9%) on Ci, whereas Cul1-Slimb-based E3 ligase added both K11-linked (48.2%) and K48-linked (41.8%) ubiquitin chains on Ci (Figure 4B). K11-linked and K48-linked ubiquitin chains are both involved in protein degradation, and these data suggest that differential ubiquitin modification of Ci may dictate the mode of protein degradation.

To determine the types of ubiquitin chains added on Ci by different E3 ligases, we next performed an in vivo ubiquitination assay using different tagged Ub mutants: V5-Ub-K11 and HA-Ub-K48, in which all lysine residues except the 11th or 48th position are mutated to arginine, respectively. We found that although Cul1-Slimb-based E3 ligase preferred to add K11-linked ubiquitin chains on Ci, Cul3-Rdx-based E3 ligase mainly added K48-linked ubiquitin chains on Ci (Figure 4C). Together, these results indicate that Cul1-Slimb and Cul3-Rdx-based E3 ligases modify Ci using different types of polyubiquitin chains.

(D and D′) A wing disc expressing *Ter94* RNAi with *AG4-Dicer2-GFP* was immunostained to show the expression of Ci (red) and GFP (green). Cells expressing *Ter94* RNAi were marked by GFP. *Ter94* knockdown resulted in a dramatic (arrows) or mild (arrowheads) elevation of Ci.
(E–F″) Low (E and E′) and high (F and F″) magnifications of wing disc carrying *Ter94^{k15502}* clones was immunostained to show the expression of Ci (red) and CD2 (green). *Ter94^{k15502}* clones are recognized by the lack of CD2 and dashed lines to show the boundary of clones. Ter94 mutant cells (arrows) exhibit elevated Ci levels.
(G–G‴) A wing disc expressing *Ter94* RNAi with *AG4-Dicer2* was immunostained with Ci (red), CD2 (green), and β-galactosidase (blue) antibodies. *Ter94* knockdown (marked by the lack of CD2, arrows) resulted in an elevation of Ci protein levels, but not the transcription of *ci-lacZ* (G‴).
(H and I) An eye disc expressing *Ter94* RNAi with *AG4-Dicer2* was immunostained to show Ci (red) and CD2 (green). (I) is an enlarged view of (H). Ci only accumulated in the region of *Ter94* knockdown cells anterior to the MF.
(J and K) Low (J) and high (K) magnifications of an eye disc expressing *UAS-Ter94^{AA}-V5* mutants with *AG4* was immunostained to show Ci (red) and V5 tag (green). Ci only accumulated in the cells anterior to the MF of Ter94^{AA} overexpressing clones.
(L) Western blot analysis of immunoprecipitates or lysates from wing discs expressing HA-Ci155 alone or HA-Ci155 plus *Ter94* RNAi using *MS1096-Dicer2* driver. Approximately 200 wing discs were dissected, lysed, and immunoprecipitated with HA antibody and then blotted with HA antibody. To compare the ratio of Ci155 to Ci75, the loading amounts of immunoprecipitates were adjusted according to Ci155 protein level. Intensity ratio of Ci155 to Ci75 of each lane was indicated below.
(M and N) Low (M) and high (N) magnifications of wing disc carrying *Ter94^{k15502}* clones was immunostained to show the expression of *dpp-lacZ* (red) and CD2 (green). *Ter94^{k15502}* clones are recognized by the lack of CD2 and dashed lines to show the boundary of clones. Ter94 mutant cells exhibit elevated *dpp-lacZ* levels.
(O) Western blots of whole cell lysates from NIH/3T3 cells transfected with control RNAi or *p97* RNAi with indicated antibodies. Intensity ratio of Gli3^{FL} to Gli3^{R} of each lane was indicated below.
See also Figure S1.

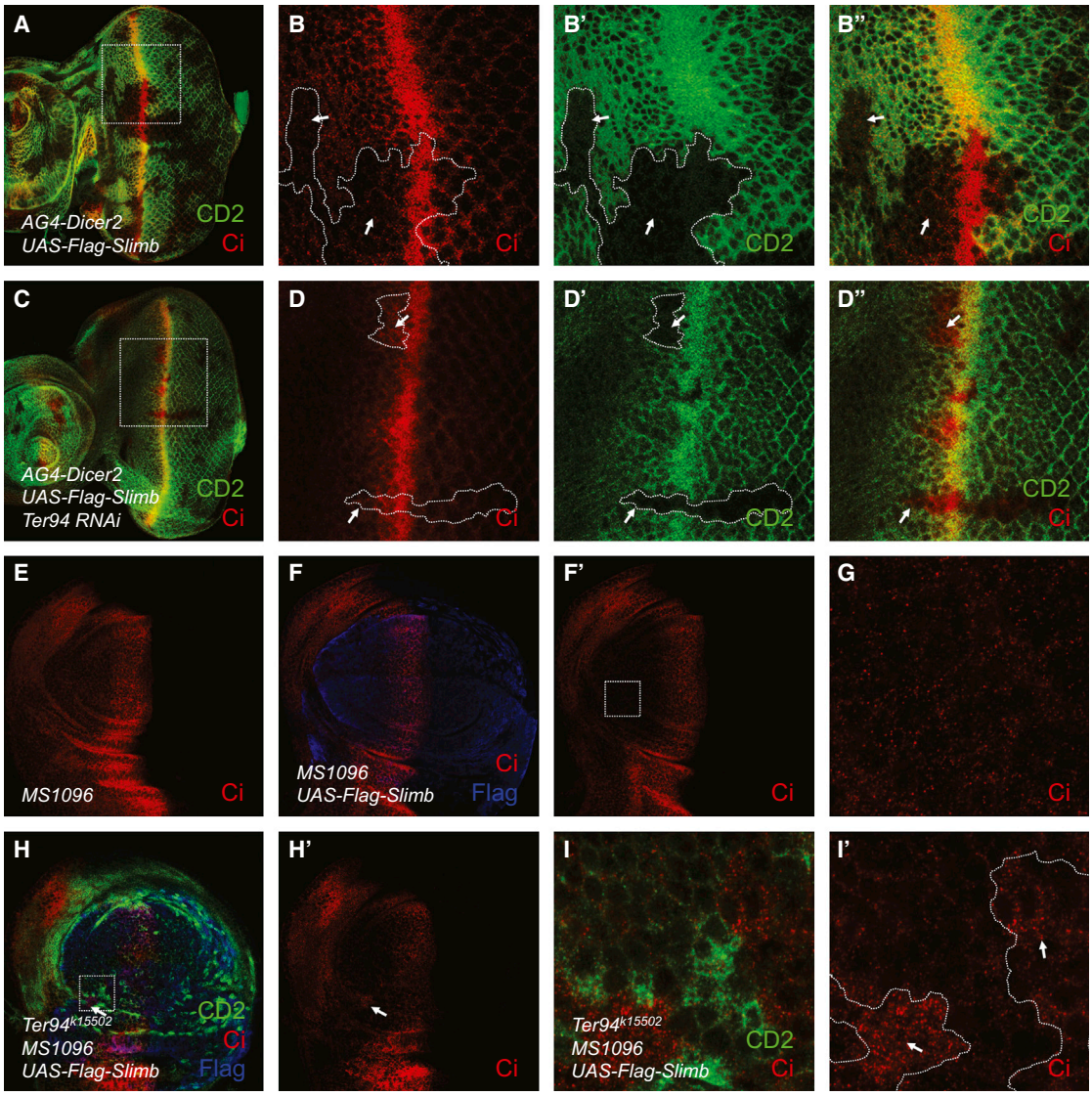

Figure 2. Loss-of-Ter94 Function Blocks Ci Degradation by Cul1-Slimb-Based E3 Ligase

(A–D″) Low (A and C) and high (B–B″ and D–D″) magnification views of eye discs expressing *UAS-Flag-Slimb* alone (A–B″) or *UAS-Flag-Slimb/Ter94* RNAi (C–D″) together with *AG4-Dicer2* were immunostained with Ci (red) and CD2 (green) antibodies. Overexpression of Slimb caused downregulation of Ci in the cells anterior to the MF (arrows in B–B″, marked by lack of CD2). *Ter94* knockdown blocked the degradation of Ci by Slimb (arrows in D–D″, marked by lack of CD2). (E) A *MS1096* wing disc was immunostained to show Ci (red).

(F–I′) Wing discs expressing *UAS-Flag-Slimb* alone or *UAS-Flag-Slimb/Ter94*^{k15502} together by *MS1096* were immunostained to show Ci (red), CD2 (green), and Flag tag (blue). (G) is an enlarged view of region marked by dashed lines in (F′). (I) and (I′) are enlarged views of region marked by dashed lines in (H). Ci also accumulated in *Ter94*^{k15502} clones (marked by lack of CD2) when Slimb was overexpressed at the same time. Arrows pointed at the accumulated Ci in *Ter94*^{k15502} clones (H, H′, and I′).

See also Figure S2.

K11-Linked Ubiquitin Chains Play a Specific Role in Cul1-Slimb-Mediated Degradation of Ci, but Not Arm

To investigate whether K11-linked ubiquitin chains play a specific role in Ter94-mediated Ci degradation, we performed immunostaining of wing discs using K11 (Matsumoto et al., 2010) or K48 (Newton et al., 2008) linkage-specific antibodies (see verification of antibodies in Figures S5A–S5F). *Ter94* or *Slimb* RNAi expression was driven by *Ci-Gal4-Dicer2* in the anterior compartment of wing disc. In *Ter94* knockdown wing discs, levels of Ci155 as well as K11-linked ubiquitin chains were elevated dramatically in the same region (Figures S5H–S5H′ compared to Figures S5G–S5G′), whereas levels of K48-linked ubiquitin chains were largely unaffected (Figure S5K compared to Figure S5J). In contrast, although Ci155 levels were elevated in *Slimb* knockdown wing discs (Figure S5I), the levels of both K11- or K48-linked ubiquitin chains were not altered (Figures S5I′ and S5L). Consistent with this result, in Kc167 cells, K11-linked ubiquitinated Ci increased upon *Ter94* knockdown whereas *Slimb* knockdown resulted in a reduction of K11-linked ubiquitinated Ci (Figures 4D and 4D′). When *Ter94* and *Slimb*

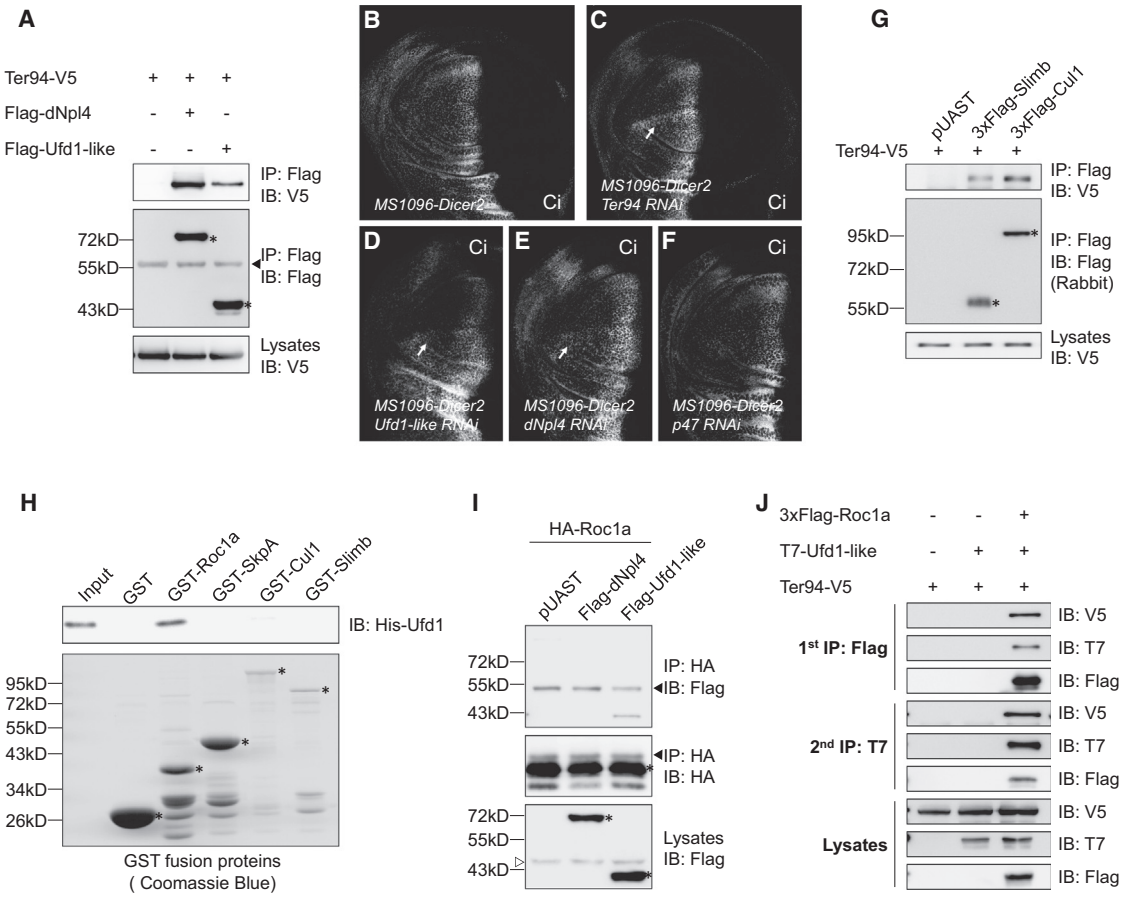

Figure 3. Ter94$^{Ufd1\text{-}like/dNpl4}$ Forms a Complex with Cul1-Slimb-Based E3 Ligase through Ufd1-like and Roc1a

(A) Western blots of immunoprecipitates (top two panels) or lysates (bottom) from S2 cells expressing indicated proteins.

(B–F) Wing discs expressing *Ter94* RNAi (C), *Ufd1-like* RNAi (D), *dNpl4* RNAi (E) or *p47* RNAi (F) with *MS1096-Dicer2* were immunostained to show Ci. Knockdown of each components of the Ter94$^{Ufd1\text{-}like/dNpl4}$ complex led to the accumulation of Ci (arrows), whereas *p47* knockdown failed to affect Ci level.

(G) Western blots of immunoprecipitates (top two panels) or lysates (bottom) from S2 cells expressing indicated proteins.

(H) Purified His-tagged Ufd1-like (His-Ufd1-like) was incubated with GST or indicated GST-tagged proteins. The bound proteins were analyzed by western blot using His antibody (top). The amounts of GST and GST fusion proteins were visualized by Coomassie blue staining (bottom).

(I) Western blots of immunoprecipitates (top two panels) or lysates (bottom) from S2 cells expressing indicated proteins.

(J) S2 cells expressing the indicated proteins were harvested for the two-step immunoprecipitation (2-step IP) and analyzed by western blot.

In all blots, asterisks indicate positions of each proteins, arrowheads indicate IgG, and the open arrowhead indicates nonspecific bands.

See also Figure S3.

were knockdown together, the levels of K11-linked ubiquitinated Ci decreased dramatically compared with control RNAi. These results suggest that *Ter94* knockdown leads to accumulation of K11-linked ubiquitinated Ci, which is dependent on the function of Slimb.

We also examined the knockdown effects of *Ter94* on the degradation of Armadillo (Arm), which is another substrate of Cul1-Slimb-based E3 ligase and undergoes complete proteasomal degradation (Jiang and Struhl, 1998; Ou et al., 2002). Interestingly, we found that knockdown of *Ter94* does not increase the protein level of Arm (Figure S4F), suggesting a specific involvement of Ter94 in the regulation of Ci degradation by Cul1-Slimb-based E3 ligase. In vivo ubiquitination experiments revealed that Cul1-Slimb mainly added K48-linked ubiquitin chains on Arm, but not K11-linked ubiquitin chains (Figure S4G). The differential ubiquitin modification of Ci and Arm by Cul1-Slimb-based E3 ligase (Figures S4H and S4I) provides indirect evidence supporting the specific involvement of K11-linked ubiquitin chains on Ci is linked to partial degradation by proteasomes.

Ter94$^{Ufd1\text{-}like/dNpl4}$ Prefers K11-Linked Ubiquitinated Ci

Previous studies have shown that the p97$^{Ufd1/Npl4}$ complex binds ubiquitinated proteins via the Npl4 (Meyer et al., 2002) or Ufd1 (Ye et al., 2003). Using polyubiquitinated substrates and purified GST-Ufd1-like or GST-dNpl4, we found that dNpl4 of the Ter94 complex has a high affinity with polyubiquitin chains, compared with Ufd1-like (Figure 4E). Next, we tested whether Ter94$^{Ufd1\text{-}like/dNpl4}$ complex selects ubiquitinated Ci generated by Cul1-Slimb or Cul3-Rdx-based E3 ligase using a method described in Figure 4F (see detailed description in Supplemental Experimental Procedures). The results revealed that Ci was highly ubiquitinated in the ATP+, but not the ATP−, group and that

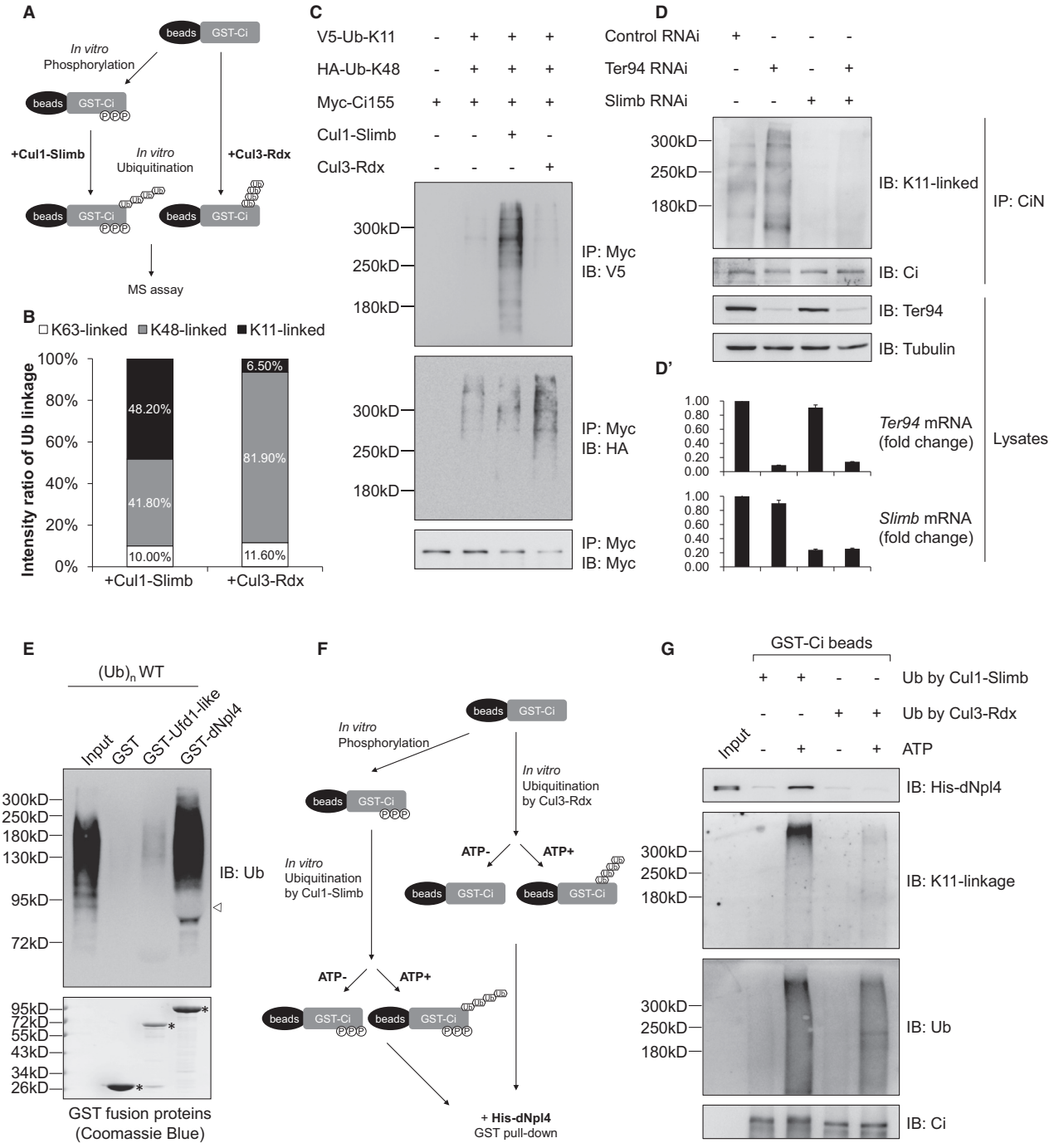

Figure 4. dNpl4 of Ter94$^{Ufd1\text{-}like/dNpl4}$ Complex Favors K11-Linked Ubiquitinated Ci by Cul1-Slimb-Based E3 Ligase

(A) A schematic of the procedures used for the generation of ubiquitinated GST-Ci for mass spectrometry.

(B) Statistic analysis of mass spectrometry samples from in vitro ubiquitinated GST-Ci by Cul1-Slimb or Cul3-Rdx-based E3 ligase.

(C) Western blots of in vivo ubiquitination of Ci.

(D and D′) Kc167 cells were treated with indicated dsRNA and harvested for immunoprecipitation with CiN antibody and analyzed by western blot. To compare the ubiquitination level, the loading amounts were adjusted according to Ci protein level. An aliquot of cell lysates was used for RNA preparation and real-time PCR to verify the RNAi efficiency (D′) Data are represented as mean ± SD, n = 4.

(E) Western blot of GST pull-down assay. The amounts of GST and GST fusion proteins were visualized with Coomassie blue staining (bottom). Asterisks indicate positions of GST-fusion proteins. The open arrowhead indicates excessive GST protein detected on the film.

(F) A flow chart shows the experimental procedures used to test the binding between ubiquitinated GST-Ci and His-dNpl4.

(G) Western blots of GST pull-down results indicated in (F).

See also Figures S4 and S5.

dNpl4 bound specifically with ubiquitinated Ci by Cul1-Slimb, but not Cul3-Rdx (Figure 4G). The total ubiquitination level of ATP+ groups between Cul1-Slimb and Cul3-Rdx is comparable as revealed by anti-ubiquitin antibody, but K11-linkage signal is much higher in Cul1-Slimb ATP+ group than Cul3-Rdx ATP+ group. To further investigate the ubiquitin linkage that mediates the interactions of ubiquitinated Ci with the Ter94 complex, we performed coIP experiments in the presence of Ub Lys11 to Arg (K11R) or Lys48 to Arg (K48R) mutants. As shown in Figure S5M, Ub-K11R specifically reduced the binding of Ter94 to Ci. Taken together, these data demonstrate that Ter94 complex binds ubiquitinated Ci by Cul1-Slimb-based E3 ligase through K11-linked ubiquitination.

DISCUSSION

The control of partial versus complete proteasomal degradation of Ci and Gli3 is a major regulatory step in Hh signal transduction (Hui and Angers, 2011). How proteasomes distinguish ubiquitinated Ci to carry out either partial or complete degradation is not known. Based on our findings, we propose the following model. In the absence of Hh, Ci155 is phosphorylated and ubiquitinated by Cul1-Slimb-based E3 ligase to generate Ci75. In this process, K11-linked ubiquitin chains are added onto Ci155. Ter94$^{Ufd1\text{-}like/dNpl4}$ forms a complex with Cul1-Slimb-based E3 ligase through Ufd1-like and Roc1a, and another component dNpl4 is bound to the K11-linked ubiquitin chains on Ci155. Through ATP hydrolysis, Ter94$^{Ufd1\text{-}like/dNpl4}$ facilitates the delivery of ubiquitinated Ci155 to the proteasomes for processing.

Besides Ci and Gli3, the best example of partial degradation is the processing of human nuclear factor-κB (NF-κB) (Palombella et al., 1994) and its yeast homologs, SPT23 and MGA2 (Hoppe et al., 2000; Rape et al., 2001). Previous studies have suggested that some common features of processing determinant domain (PDD) are involved in the partial proteasomal degradation of Ci and NF-κB (Tian et al., 2005). However, Ci also undergoes complete proteasomal degradation by Cul3-Rdx-based E3 ligase (Kent et al., 2006; Zhang et al., 2006). Why such ''degradation stop signals'' fail to work in such instances and how proteasomes make the decision for partial or complete degradation are unknown. Based on our results and previous studies, we propose that Ter94/p97 complex may specifically target ''partial-degradation-proteins'' to proteasomes through K11-linked ubiquitin chains. Further investigation is needed to provide direct evidence to support this hypothesis. As many similarities are shared between Ci and NF-κB precursors in partial degradation, it will be interesting to test whether p97 and K11-linked ubiquitination are also involved in the partial degradation and/or maturation of p100 in NF-κB signaling.

In this study, we found that K11-linked chains are added onto Ci by Cul1-Slimb-based E3 ligase in the absence of Hh pathway activity, whereas Cul3-Rdx-based E3 ligase mainly adds K48-linked chains on Ci when the pathway is active. This illustrates a phenomenon that the same protein can be modified with different types of ubiquitin chains by distinct E3 ligases. Although K11-linked chains added on APC substrates lead to complete degradation (Jin et al., 2008; Matsumoto et al., 2010), our data demonstrate that K11-linked chains are involved in the partial degradation of Ci. Our findings also raise the interesting possibility that the topology of ubiquitin chains may be recognized as a selective signal for proteasomal degradation. As mixed or heterologous ubiquitin chains may exist (Ikeda and Dikic, 2008), further investigation is essential to determine whether mixed ubiquitin chains are formed by Cul1-Slimb-based E3 ligase on Ci.

EXPERIMENTAL PROCEDURES

Immunostaining of imaginal discs, GST fusion protein pull-down, mammalian cell culture, and mass spectrometry analysis of ubiquitin linkage were performed according to standard protocols. For detailed procedures and fly strains used in this study, see the Supplemental Experimental Procedures.

Drosophila Cell Culture, RNAi, Transfection, Immunoprecipitation, and Western Blot Analysis

S2 and Kc167 cells were cultured at 25°C in Schneider's *Drosophila* Medium (Invitrogen) with 10% fetal bovine serum, 100 U/ml of penicillin, and 100 μg/ml of streptomycin. To perform dsRNA-mediated knockdown experiment, Kc167 cells were diluted into 1 × 10^6 cells/ml and mixed with 15 μg dsRNA per 1 × 10^6 cells for 1 hr starvation in serum free medium. Transfection was carried out by using a Calcium Phosphate Transfection Kit (Specialty Media) according to manufacturer's instructions. Forty-eight hours after transfection, cells were harvested with indicated buffers for different assays. For two-step immunoprecipitation in Figure 3J, anti-Flag M2 affinity gel (Sigma) was used to purify 3xFlag-Roc1a complex in the first-step immunoprecipitation (first IP). Beads from the first IP were eluted with 3xFlag peptide (Sigma) and then mixed with anti-T7 antibody to purify T7-Ufd1-like complex in the second-step immunoprecipitation (second IP). Western blot was performed according to standard protocol. See Supplemental Experimental Procedures for antibodies used and other details.

In Vivo Ubiquitination, In Vitro Phosphorylation, and Ubiquitination Assay

In vivo ubiquitination assay was performed as previously described (Zhang et al., 2006) (Supplemental Experimental Procedures). To create recognition sites for Cul1-Slimb-based E3 ligase, GST-Ci155-loaded beads purified from *E. coli* were incubated with 500 U CKI, 1,250 U PKA, and 250 U GSK3 (NEB) in GSK3 reaction buffer (20 mM Tris-Cl pH 7.5, 10 mM magnesium chloride, 5 mM DTT, 1 mM ATP) at 30°C for 30 min. For in vitro ubiquitination assay, GST-Ci155 beads were incubated with 100 ng E1 (Rabbit), 200 ng E2 (UbcH5c), 5 μg ubiquitin (Boston Biochem), 2 mM ATP, and E3 complex in 20 μl ubiquitination buffer (50 mM Tris-Cl pH 7.5, 5 mM magnesium chloride, 2 mM sodium fluoride, 0.6 mM DTT, 10 nM Okadaic acid) at 30°C for 2 hr. E3 (Cul1-Slimb or Cul3-Rdx) complex was immunoprecipitated from S2 cells expressing 3xFlag-tagged Slimb or Rdx complex and eluted by 3xFlag peptides (Sigma).

SUPPLEMENTAL INFORMATION

Supplemental Information includes Supplemental Experimental Procedures and five figures and can be found with this article online at http://dx.doi.org/10.1016/j.devcel.2013.05.006.

ACKNOWLEDGMENTS

We are grateful to Dr. Mary Ann Price for providing Kc167 cells. We thank Drs. Thomas Kornberg, Jin Jiang, Lin Li, Yihong Ye, Cheng-Ting Chien, Baolin Wang, Pao-Tien Chuang, Chao Tong, and Dahua Chen and DSHB, VDRC, NIG, and the Bloomington Stock Center for fly stocks and reagents. We thank Drs. Rong Zeng and Chen Li for helping with mass spectrometry assay. We also thank Drs. Lin Li, Min Wu, Yingzi Yang, Zhengfan Jiang, Zhaocai Zhou, and Jinqiu Zhou for discussions and comments on the manuscript. This work was supported by grants from the National Basic Research Program of China (973 Program: 2011CB943902, 2010CB912101, and 2012CB945001), the National Natural Science Foundation of China (31171414 and 31171394), and the "Strategic Priority Research Program" of the Chinese Academy of

Sciences (XDA01010405 and XDA01010406) to Y.Z. and L.Z., as well as grants from the Canadian Cancer Society to C.-c.H.

Received: April 6, 2012
Revised: April 9, 2013
Accepted: May 3, 2013
Published: June 6, 2013

REFERENCES

Alexandru, G., Graumann, J., Smith, G.T., Kolawa, N.J., Fang, R., and Deshaies, R.J. (2008). UBXD7 binds multiple ubiquitin ligases and implicates p97 in HIF1alpha turnover. Cell *134*, 804–816.

Aza-Blanc, P., Ramírez-Weber, F.A., Laget, M.P., Schwartz, C., and Kornberg, T.B. (1997). Proteolysis that is inhibited by hedgehog targets Cubitus interruptus protein to the nucleus and converts it to a repressor. Cell *89*, 1043–1053.

Cardozo, T., and Pagano, M. (2004). The SCF ubiquitin ligase: insights into a molecular machine. Nat. Rev. Mol. Cell Biol. *5*, 739–751.

Chen, M.H., Wilson, C.W., and Chuang, P.T. (2007). SnapShot: hedgehog signaling pathway. Cell *130*, 386.

Donaldson, T.D., Noureddine, M.A., Reynolds, P.J., Bradford, W., and Duronio, R.J. (2004). Targeted disruption of Drosophila Roc1b reveals functional differences in the Roc subunit of Cullin-dependent E3 ubiquitin ligases. Mol. Biol. Cell *15*, 4892–4903.

Eaton, S., and Kornberg, T.B. (1990). Repression of ci-D in posterior compartments of Drosophila by engrailed. Genes Dev. *4*, 1068–1077.

Haglund, K., and Dikic, I. (2005). Ubiquitylation and cell signaling. EMBO J. *24*, 3353–3359.

Hartmann-Petersen, R., Seeger, M., and Gordon, C. (2003). Transferring substrates to the 26S proteasome. Trends Biochem. Sci. *28*, 26–31.

Henne, W.M., Buchkovich, N.J., and Emr, S.D. (2011). The ESCRT pathway. Dev. Cell *21*, 77–91.

Hooper, J.E., and Scott, M.P. (2005). Communicating with Hedgehogs. Nat. Rev. Mol. Cell Biol. *6*, 306–317.

Hoppe, T., Matuschewski, K., Rape, M., Schlenker, S., Ulrich, H.D., and Jentsch, S. (2000). Activation of a membrane-bound transcription factor by regulated ubiquitin/proteasome-dependent processing. Cell *102*, 577–586.

Hui, C.C., and Angers, S. (2011). Gli proteins in development and disease. Annu. Rev. Cell Dev. Biol. *27*, 513–537.

Ikeda, F., and Dikic, I. (2008). Atypical ubiquitin chains: new molecular signals. 'Protein Modifications: Beyond the Usual Suspects' review series. EMBO Rep. *9*, 536–542.

Jia, J., Amanai, K., Wang, G., Tang, J., Wang, B., and Jiang, J. (2002). Shaggy/GSK3 antagonizes Hedgehog signalling by regulating Cubitus interruptus. Nature *416*, 548–552.

Jiang, J., and Struhl, G. (1998). Regulation of the Hedgehog and Wingless signalling pathways by the F-box/WD40-repeat protein Slimb. Nature *391*, 493–496.

Jiang, J., and Hui, C.C. (2008). Hedgehog signaling in development and cancer. Dev. Cell *15*, 801–812.

Jin, L., Williamson, A., Banerjee, S., Philipp, I., and Rape, M. (2008). Mechanism of ubiquitin-chain formation by the human anaphase-promoting complex. Cell *133*, 653–665.

Juhász, G., Hill, J.H., Yan, Y., Sass, M., Baehrecke, E.H., Backer, J.M., and Neufeld, T.P. (2008). The class III PI(3)K Vps34 promotes autophagy and endocytosis but not TOR signaling in Drosophila. J. Cell Biol. *181*, 655–666.

Kent, D., Bush, E.W., and Hooper, J.E. (2006). Roadkill attenuates Hedgehog responses through degradation of Cubitus interruptus. Development *133*, 2001–2010.

Kondo, H., Rabouille, C., Newman, R., Levine, T.P., Pappin, D., Freemont, P., and Warren, G. (1997). p47 is a cofactor for p97-mediated membrane fusion. Nature *388*, 75–78.

Matsumoto, M.L., Wickliffe, K.E., Dong, K.C., Yu, C., Bosanac, I., Bustos, D., Phu, L., Kirkpatrick, D.S., Hymowitz, S.G., Rape, M., et al. (2010). K11-linked polyubiquitination in cell cycle control revealed by a K11 linkage-specific antibody. Mol. Cell *39*, 477–484.

Méthot, N., and Basler, K. (1999). Hedgehog controls limb development by regulating the activities of distinct transcriptional activator and repressor forms of Cubitus interruptus. Cell *96*, 819–831.

Meyer, H., Bug, M., and Bremer, S. (2012). Emerging functions of the VCP/p97 AAA-ATPase in the ubiquitin system. Nat. Cell Biol. *14*, 117–123.

Meyer, H.H., Wang, Y., and Warren, G. (2002). Direct binding of ubiquitin conjugates by the mammalian p97 adaptor complexes, p47 and Ufd1-Npl4. EMBO J. *21*, 5645–5652.

Motzny, C.K., and Holmgren, R. (1995). The Drosophila cubitus interruptus protein and its role in the wingless and hedgehog signal transduction pathways. Mech. Dev. *52*, 137–150.

Murphy, T.D. (2003). Drosophila skpA, a component of SCF ubiquitin ligases, regulates centrosome duplication independently of cyclin E accumulation. J. Cell Sci. *116*, 2321–2332.

Newton, K., Matsumoto, M.L., Wertz, I.E., Kirkpatrick, D.S., Lill, J.R., Tan, J., Dugger, D., Gordon, N., Sidhu, S.S., Fellouse, F.A., et al. (2008). Ubiquitin chain editing revealed by polyubiquitin linkage-specific antibodies. Cell *134*, 668–678.

Noureddine, M.A., Donaldson, T.D., Thacker, S.A., and Duronio, R.J. (2002). Drosophila Roc1a encodes a RING-H2 protein with a unique function in processing the Hh signal transducer Ci by the SCF E3 ubiquitin ligase. Dev. Cell *2*, 757–770.

Ou, C.Y., Lin, Y.F., Chen, Y.J., and Chien, C.T. (2002). Distinct protein degradation mechanisms mediated by Cul1 and Cul3 controlling Ci stability in Drosophila eye development. Genes Dev. *16*, 2403–2414.

Palombella, V.J., Rando, O.J., Goldberg, A.L., and Maniatis, T. (1994). The ubiquitin-proteasome pathway is required for processing the NF-kappa B1 precursor protein and the activation of NF-kappa B. Cell *78*, 773–785.

Pintér, M., Jékely, G., Szepesi, R.J., Farkas, A., Theopold, U., Meyer, H.E., Lindholm, D., Nässel, D.R., Hultmark, D., and Friedrich, P. (1998). TER94, a Drosophila homolog of the membrane fusion protein CDC48/p97, is accumulated in nonproliferating cells: in the reproductive organs and in the brain of the imago. Insect Biochem. Mol. Biol. *28*, 91–98.

Price, M.A., and Kalderon, D. (2002). Proteolysis of the Hedgehog signaling effector Cubitus interruptus requires phosphorylation by Glycogen Synthase Kinase 3 and Casein Kinase 1. Cell *108*, 823–835.

Rape, M., Hoppe, T., Gorr, I., Kalocay, M., Richly, H., and Jentsch, S. (2001). Mobilization of processed, membrane-tethered SPT23 transcription factor by CDC48(UFD1/NPL4), a ubiquitin-selective chaperone. Cell *107*, 667–677.

Richly, H., Rape, M., Braun, S., Rumpf, S., Hoege, C., and Jentsch, S. (2005). A series of ubiquitin binding factors connects CDC48/p97 to substrate multiubiquitylation and proteasomal targeting. Cell *120*, 73–84.

Simpson, P. (1979). Parameters of cell competition in the compartments of the wing disc of Drosophila. Dev. Biol. *69*, 182–193.

Tian, L., Holmgren, R.A., and Matouschek, A. (2005). A conserved processing mechanism regulates the activity of transcription factors Cubitus interruptus and NF-kappaB. Nat. Struct. Mol. Biol. *12*, 1045–1053.

Wang, B., Fallon, J.F., and Beachy, P.A. (2000). Hedgehog-regulated processing of Gli3 produces an anterior/posterior repressor gradient in the developing vertebrate limb. Cell *100*, 423–434.

Ye, Y. (2006). Diverse functions with a common regulator: ubiquitin takes command of an AAA ATPase. J. Struct. Biol. *156*, 29–40.

Ye, Y., Meyer, H.H., and Rapoport, T.A. (2001). The AAA ATPase Cdc48/p97 and its partners transport proteins from the ER into the cytosol. Nature *414*, 652–656.

Ye, Y., Meyer, H.H., and Rapoport, T.A. (2003). Function of the p97-Ufd1-Npl4 complex in retrotranslocation from the ER to the cytosol: dual recognition of nonubiquitinated polypeptide segments and polyubiquitin chains. J. Cell Biol. *162*, 71–84.

Zhang, Q., Zhang, L., Wang, B., Ou, C.Y., Chien, C.T., and Jiang, J. (2006). A hedgehog-induced BTB protein modulates hedgehog signaling by degrading Ci/Gli transcription factor. Dev. Cell *10*, 719–729.